Eigenstate expansion of the quasistatic electric field of a point charge in a spherical inclusion structure

Asaf Farhi* and David J. Bergman†

Raymond and Beverly Sackler School of Physics and Astronomy, Faculty of Exact Sciences, Tel Aviv University, IL-69978 Tel Aviv, Israel

(Received 20 June 2017; published 3 October 2017)

A point charge in the presence of a metallic nanosphere is a fundamental setup, which has implications for Raman scattering, enhancement of spontaneous emission of a molecule by an antenna, sensing, and modeling a metallic tip in proximity to a nanoparticle. Here we analytically expand the electric field of a point charge in an ϵ_2 host medium in the presence of an ϵ_1 sphere using the sphere eigenstates, where ϵ_1 and ϵ_2 can take any complex values. We develop a simple procedure to treat charge distribution, which results in a simple eigenstate expansion for the electric field of charge sources and is able to treat volume sources analytically. The electric field is strongly enhanced when ϵ_1/ϵ_2 is close to an $(\epsilon_1/\epsilon_2)_l$ eigenvalue of a dominant mode, which is determined by the point charge location and the measurement point. An electric field exists inside the sphere when ϵ_1/ϵ_2 is close to a $(\epsilon_1/\epsilon_2)_l$ resonance even when ϵ_1 is a conductor. Low-order modes generate an electric field far away from the interface, where the $l = 1$ mode with a resonance at $\epsilon_1 = -2\epsilon_2$ generates a field at the sphere center. The high-order modes, which are associated with high spatial frequencies, become more dominant when the point charge approaches the sphere surface or when the physical parameters are close the high-order modes resonances. When ϵ_1/ϵ_2 is smaller or larger than the eigenvalues of the dominant modes, the modes interfere constructively and generate a strong signal at an angular direction equal to that of the source. The spectral information at the sphere surface may be utilized to calculate the point charge location without knowing its magnitude.

DOI: 10.1103/PhysRevA.96.043806

I. INTRODUCTION

The electrostatic potential of a point charge in proximity to a conducting sphere was calculated analytically long ago [1]. This calculation assumes a constant potential on the sphere envelope and uses the method of images to construct a potential outside the sphere. The electrostatic potential of a point charge next to a dielectric sphere with vanishing conductivity was calculated by using solutions of Laplace's equation and matching boundary conditions of the electric field [2]. The electrodynamics of surface systems has been approached using a Green's function formalism in Ref. [3]. The electromagnetic field of an oscillating dipole outside a conducting sphere has been calculated by transforming an infinite series of spherical harmonics for the Hertzian vector into a more rapidly converging series [4]. In another study the electric field of an oscillating dipole inside a dielectric sphere was calculated by expanding the field in the vector spherical harmonics and matching the field boundary conditions [5]. Radiation emission rates for such a setup, where the dipole models a molecule, were calculated, taking into account electrostatic spherical and spheroidal cavity effects [6]. Asymptotic expressions for the potential and the field very close to an interface between an inclusion and a host medium in the limit $\epsilon_1 = -\epsilon_2$, both real, have also been obtained [7–10].

In the quasistatic regime, which occurs when the typical lengths of the system are much shorter than the wavelength, Maxwell's equations reduce to Poisson's equation with a complex and frequency-dependent permittivity $\epsilon(\omega)$. To account for a nonlocal conductivity and permittivity, $\epsilon(\omega)$ should be expressed as a tensor that depends also on the wave vector $\mathbf{k}$ [1]. Metals at optical frequencies can be described using an only ω-dependent permittivity and we therefore assume this dependence in our derivations. To investigate a composite system with a source in the quasistatic regime, a point charge is often used to observe its properties. Scattering eigenstates of Maxwell's equations have been exploited to calculate the electric field in electrostatics [11–15] and in electrodynamics [16,17]. Recently, a procedure to treat current sources using the electromagnetic spectral expansion has been introduced [17].

Here we introduce a procedure to treat charge sources using the electrostatic eigenstate expansion. Such a procedure results in a simple eigenstate expansion for the electric field of charge sources and is able to treat volume sources analytically. In addition, we show that when the system is close to a resonance a strong electric field exists inside the sphere even if it is a conductor.

Potential applications are enhancement of spontaneous emission of a molecule by an antenna [18] in the quasistatic regime, modeling a tip in proximity to a metallic nanosphere, near-field imaging, sensing, and Raman spectroscopy. In particular, enhancement of Raman scattering and spontaneous emission of a molecule become more dominant when the field intensity at the molecule is higher, which can be obtained when the system is close to a resonance. Near-field imaging exploits evanescent waves to generate an image with resolution that is better than the diffraction limit. In this technique a two-dimensional image is generated by scanning the surface with a scattering tip. We show that the spectral information of the electric field can be utilized to calculate the point charge location when it is not at the sphere surface, which we define as the detector.

In Sec. II we present the theory and introduce a procedure to treat charge sources. In Sec. III we describe how we can

*asaffarhi@post.tau.ac.il
†bergman@post.tau.ac.il

 ©2017 American Physical Society

obtain the point charge location from the spectral content of the electric field on the sphere surface. In Sec. IV we present the potential and the electric field for permittivity values that are close to the resonances of the dominant eigenstates. In Sec. V we discuss our results and potential applications.

II. THEORY

In the quasistatic regime Maxwell's equations reduce to Poisson's equation with a complex and frequency-dependent permittivity

$$\nabla \cdot (\epsilon \nabla \psi) = -4\pi\rho. \tag{2.1}$$

By expressing the permittivity using the step functions θ_1 and θ_2 of the ϵ_1 and ϵ_2 media [$\theta_i(\mathbf{r}) = 1$ when $\epsilon(\mathbf{r}) = \epsilon_i$; otherwise $\theta_i(\mathbf{r}) = 0$] we write [11]

$$\begin{aligned} &\nabla \cdot [(\epsilon_1\theta_1 + \epsilon_2\theta_2)\nabla\psi] = -4\pi\rho, \\ &\nabla^2\psi = -4\pi\rho + u\nabla\cdot(\theta_1\nabla\psi), \quad u \equiv 1 - \frac{\epsilon_1}{\epsilon_2}. \end{aligned} \tag{2.2}$$

This is transformed to [11]

$$\psi = \psi_0 + u\Gamma\psi, \tag{2.3}$$

where

$$\begin{aligned} \Gamma\psi &= \int dV'\theta_1(\mathbf{r}')\nabla' G(\mathbf{r},\mathbf{r}')\cdot\nabla'\psi(\mathbf{r}'), \\ G &= \frac{1}{4\pi|\mathbf{r}-\mathbf{r}'|}, \quad \psi_0 = \frac{q}{\epsilon_2|\mathbf{r}-\mathbf{r}_0|}, \end{aligned} \tag{2.4}$$

and $\mathbf{r}_0$ is the point charge position, assumed to be in the ϵ_2 medium.

The eigenstates satisfy Eq. (2.3) when there is no source, namely,

$$s_n\psi_n = \Gamma\psi_n, \quad \frac{1}{s_n} \equiv u_n = 1 - \frac{\epsilon_{1n}}{\epsilon_2}. \tag{2.5}$$

By defining the scalar product

$$\langle\psi|\phi\rangle \equiv \int dV\,\theta_1\nabla\psi^*\cdot\nabla\phi, \tag{2.6}$$

Γ becomes a Hermitian operator and therefore it has a complete set of eigenstates. We insert the unity operator in Eq. (2.3) and arrive at

$$\psi = \psi_0 + \sum_n \frac{s_n}{s-s_n}\langle\psi_n|\psi_0\rangle\psi_n, \quad s \equiv 1/u, \tag{2.7}$$

where ψ_n are the normalized eigenstates.

The sphere eigenstates are [11]

$$\psi_n \equiv \psi_{lm}(\mathbf{r}) = \frac{Y_{lm}(\Omega)}{(la)^{1/2}} \times \begin{cases} \left(\frac{r}{a}\right)^l, & r < a \\ \left(\frac{a}{r}\right)^{l+1}, & r > a, \end{cases} \tag{2.8}$$

where a is the sphere radius, Y_{lm} are the spherical harmonics, and the eigenvalues are

$$\epsilon_{1l} = -\epsilon_2\frac{l+1}{l}, \quad s_{lm} \equiv s_l = \frac{l}{2l+1}. \tag{2.9}$$

Clearly, in the $l \to \infty$ limit $s_l \to 1/2$. Thus, for a choice of $s \approx 1/2$ the high-order modes make a large contribution to the potential [11,12,15].

Note that the inclusion permittivity eigenvalues are real and on the order of magnitude of the host medium permittivity (with the opposite sign). In statics, the imaginary part of a metal permittivity is very high and it is impossible to approach the resonances. At high frequencies that imaginary part can become small and the resonances can be approached. In such a case, the physical electric field becomes very large due to a high contribution of one of the modes in the eigenstate expansion. The coefficient of an eigenstate $s_l^2/(s-s_l)$ can be expressed as

$$\frac{s_l^2}{s-s_l} = \frac{s_l^2/s}{1 - s_l(1-\epsilon_1/\epsilon_2)}$$

and becomes large when the real and imaginary parts of the denominator $1 - s_l(1-\epsilon_1/\epsilon_2)$ are small. Assuming $\mathrm{Im}(\epsilon_1), \mathrm{Im}(\epsilon_2) > 0$ and $\mathrm{Re}(\epsilon_1) < 0$, $\mathrm{Im}(\epsilon_1)$ and $\mathrm{Im}(\epsilon_2)$ are required to be small with respect to $|\epsilon_2|^2/\mathrm{Re}(\epsilon_2)$ and $|\epsilon_2|^2/|\mathrm{Re}(\epsilon_1)|$, respectively, in order for the imaginary part of the denominator to be small. When one of the constituents has gain [14] we can approach the condition for vanishing imaginary part of the denominator $\mathrm{Im}(\epsilon_1)/\mathrm{Im}(\epsilon_2) = \mathrm{Re}(\epsilon_1)/\mathrm{Re}(\epsilon_2)$.

Now we proceed to calculate the scalar product $\langle\psi_{lm}|\psi_0\rangle$. We exploit the fact that $\psi_0(\mathbf{r}) = 4\pi/\epsilon_2\int G(\mathbf{r},\mathbf{r}')\rho(\mathbf{r}')dV'$ and use Eq. (2.5) to obtain

$$\begin{aligned} \langle\psi_{lm}|\psi_0\rangle &= \frac{4\pi}{\epsilon_2}\int\int \theta_1\nabla\psi_{lm}^*\cdot\nabla G(\mathbf{r},\mathbf{r}')\rho(\mathbf{r}')dV'dV \\ &= \frac{4\pi}{\epsilon_2}s_l\int\psi_{lm}^*(\mathbf{r}')\rho(\mathbf{r}')dV' \\ &= \frac{4\pi q}{\epsilon_2}s_l\psi_{lm}^*(\mathbf{r}_0), \end{aligned} \tag{2.10}$$

where we assumed a point charge $\rho = q\delta^3(\mathbf{r}-\mathbf{r}_0)$. We finally get

$$\psi(\mathbf{r}) = \psi_0(\mathbf{r}) + \frac{4\pi q}{\epsilon_2}\sum_{l,m}\frac{s_l^2}{s-s_l}\psi_{lm}^*(\mathbf{r}_0)\psi_{lm}(\mathbf{r}). \tag{2.11}$$

It can readily be seen from Eqs. (2.8) and (2.11) that as the point charge approaches the sphere surface the contribution of the high-order modes becomes non-negligible [because $\psi_{lm}^*(\mathbf{r}_0)$ is larger] and they become more dominant in the expansion. In addition, low-order modes decay more slowly away from the interface and can therefore generate fields far away from the interface.

The ratio ϵ_1/ϵ_2 can be chosen to enhance a contribution to the electric field of one or more modes. We can therefore decompose each term in the sum in Eq. (2.11) into $(4\pi q/\epsilon_2)s_l^2\psi_{lm}^*(\mathbf{r}_0)\psi_{lm}(\mathbf{r})$, which does not depend on s, and $1/(s-s_l)$, which is determined by the distance between the physical s and an eigenvalue s_l.

For a point charge at $\mathbf{r}_0 = z_0\hat{\mathbf{z}}$, $\psi_{lm}^*(\mathbf{r}_0) = \psi_{lm}(\mathbf{r}_0)$ and $\psi_{lm}(\mathbf{r}_0) \neq 0$ only when $m = 0$. Thus, $\psi(\mathbf{r})$ is independent of the azimuthal angle ϕ and the sum in Eq. (2.11) is considerably simplified. In addition, it can be seen that when the ratio ϵ_1/ϵ_2 is fixed, $\psi(\mathbf{r})/\psi_0(\mathbf{r})$ is also fixed since s does not

change and ϵ_2 cancels out. Therefore, the relative effect of a sphere inclusion on the potential and the electric field does not change when keeping this ratio fixed, even when ϵ_1 is large. For example, the $l=1$ resonance occurs when $\epsilon_1 \approx -2\epsilon_2$. If $\mathrm{Re}(\epsilon_1) \approx -2\,\mathrm{Re}(\epsilon_2)$ and ϵ_1 and ϵ_2 have small dissipation we will be close to the resonance. When downscaling the system by a factor b we get that $|\mathbf{E}|^2$ increases by a factor of b^4, as is the case for a point charge in a uniform medium.

To verify our result in Eq. (2.11) we placed a point charge at $\mathbf{r}_0 = z_0\hat{\mathbf{z}}$ ($z_0 > a$) and took the $\epsilon_1 \to \infty$ limit, assuming ϵ_2 is finite. We then summed a geometric series to obtain the known textbook result for $\mathbf{r}$ on the $+z$ axis

$$\psi(\mathbf{r}) = \psi_0(\mathbf{r}) - \frac{qa/z_0}{|r - a^2/z_0|}. \tag{2.12}$$

We also took the limit of a point charge near a plane. Assuming $r \approx z_0 \approx a$ and defining $k \equiv l/a$ and $z \equiv r$ we obtained

$$\left(\frac{r}{a}\right)^l \quad r < a \approx e^{-k(a-z)}, \quad \left(\frac{a}{r}\right)^{l+1} \quad r > a \approx e^{-k(z-a)},$$
$$\left(\frac{a}{z_0}\right)^{l+1} \quad z_0 > a \approx e^{-k(z_0-a)}, \quad s_k \approx \frac{1}{2}(1 - e^{-2ka}). \tag{2.13}$$

From symmetry considerations one can obtain for the eigenstates dependence on the directions parallel to the plane $\psi_{\mathbf{k}}(\boldsymbol{\rho},z) = \exp(i\mathbf{k}\cdot\boldsymbol{\rho}) f_k(z)$, where $\boldsymbol{\rho}$ is the radial vector in cylindrical coordinates and $\mathbf{k} \equiv (k_x,k_y)$. In this limit the spectrum of eigenvalues is continuous and there is an accumulation point of the eigenvalues at $s = 1/2$ [11,12,15]. Note that the eigenstates can be normalized according to Eq. (2.6) due to their exponential dependence on the direction perpendicular to the plane.

The electric field can be written as

$$\mathbf{E}(\mathbf{r}) = -\nabla\psi_0(\mathbf{r}) - \mathbf{E}_{\mathrm{scat}}, \tag{2.14}$$

where

$$\mathbf{E}_{\mathrm{scat}} \equiv -\frac{4\pi q}{\epsilon_2}\sum_l \frac{s_l^2}{s - s_l}\psi^*_{lm}(\mathbf{r}_0)\nabla\psi_{lm}(\mathbf{r}); \quad \nabla\psi_{lm}(\mathbf{r}) = \mathbf{e}_r Y_{lm}\frac{\partial f_l(r)}{\partial r} + \mathbf{e}_\phi \frac{f_l(r)}{r\sin\theta} im Y_{lm} + \mathbf{e}_\theta \frac{f_l(r)}{r}\frac{\partial Y_{l,m}}{\partial\theta};$$

$$f_l(r) = \frac{1}{(la)^{1/2}} \times \begin{cases} \left(\frac{r}{a}\right)^l, & r < a \\ \left(\frac{a}{r}\right)^{l+1}, & r > a; \end{cases} \quad \frac{\partial f_l(r)}{\partial r} = \frac{1}{(la)^{1/2}} \times \begin{cases} l\left(\frac{r}{a}\right)^l \frac{1}{r}, & r < a \\ -(l+1)\left(\frac{a}{r}\right)^{l+1}\frac{1}{r}, & r > a; \end{cases} \tag{2.15}$$

and where $\partial\psi_{lm}/\partial\theta$ can be written as [19]

$$\frac{\partial\psi_{lm}}{\partial\theta} = \mathbf{e}_\theta \frac{f_l(r)}{r\sin\theta}\left[\frac{l(l+1)}{[(2l+1)(2l+3)]^{1/2}}Y_{l+1,m} - \frac{l(l-1)}{[(2l-1)(2l+1)]^{1/2}}Y_{l-1,m}\right]. \tag{2.16}$$

Note also that the field of the $l=1$ mode does not vanish at the origin and extends far from the sphere surface. In addition, the spherical harmonics satisfy $Y_{l,m=0}(\theta=0) = 1$ and $Y_{l,m=0}(\theta=\pi) = \pm 1$. Hence, when s is very close to a resonance a dominant mode is excited and the intensity peaks at both $\theta = 0$ and $\theta = \pi$. The l components $E_{\mathrm{scat},r,l}$ at $\theta = 0$ have a positive sign for $s_l < s$ and a negative sign for $s_l > s$. In addition, $Y_{l,m=0}$ and $Y_{l+1,m=0}$ at $\theta = \pi$ have opposite signs, but at the transition between $s_{l'} < s$ and $s_{l'+1} > s$, $E_{\mathrm{scat},r,l'}$ and $E_{\mathrm{scat},r,l'+1}$ have the same sign because the coefficient $1/(s - s_l)$ also changes sign. Thus, when $s \approx (s_{l'} + s_{l'+1})/2$ the dominant l' and $l'+1$ modes will interfere destructively at $\theta = 0$ and constructively at $\theta = \pi$. When $s < s_l$ for every l ($s < 1/3$), which corresponds to $\epsilon_1 \gtrsim -2\epsilon_2$, all $E_{\mathrm{scat},r,l}$ at $\theta = 0$ have the same sign and they interfere constructively to generate a strong signal. In this case the low-order modes that extend far from the sphere surface are strongly enhanced. Similarly, when $s > s_l$ for every l ($s > 1/2$), which corresponds to $\epsilon_1 \lesssim -\epsilon_2$, all $E_{\mathrm{scat},r,l}$ at $\theta = 0$ interfere constructively and a strong signal is expected there. In this case the high-order modes that are associated with high spatial frequencies are strongly enhanced. When $s > s_l$ or $s < s_l$ for every l the signs of $E_{\mathrm{scat},r,l}$ alternate at $\theta = \pi$ and a relatively weak signal is expected there.

III. CALCULATING THE POINT CHARGE LOCATION FROM THE SPECTRAL CONTENT OF THE ELECTRIC FIELD

In the far field, a point in the object is mapped into a point in the image due to constructive interference, enabling 3D imaging. Near-field imaging exploits evanescent waves and achieves resolutions better than the diffraction limit. However, measuring an electric field in the near-field region produced by a point source that is not very close to the detector is usually difficult. This is since the modes decay exponentially with distance and since there can be orders of magnitude differences among electric-field intensities produced by point sources at different distances from the detector. When we are close to a resonance, the local physical field is enhanced and there is a significant field also due to point sources that are not very close to the detector (e.g., at the sphere surface). Thus, high-order components of the electric field can be detected. For a single point charge source, which we will treat as the object, the image field intensity will be maximal at an angular direction equal to that of the source and at the reflected direction with respect to the spherical surface (see Sec. II).

We start by calculating the field at the sphere surface and requiring full retrieval of an l mode of the electric field. We expand ψ_0 inside the sphere, where there are no sources, using the unity operator. We then take the gradient of Eq. (2.14) to obtain the following expression for the electric field, which is valid inside the sphere:

$$\begin{aligned}\mathbf{E}_{\text{inside}} &= -\sum_{l,m=0}\left[\langle\psi_{lm}|\psi_0\rangle\nabla\psi_{lm}+\frac{s_l}{s-s_l}\langle\psi_{lm}|\psi_0\rangle\nabla\psi_{lm}\right]\\ &= -\sum_{l,m=0}\frac{s}{s-s_l}\langle\psi_{lm}|\psi_0\rangle\nabla\psi_{lm}. \end{aligned}\tag{3.1}$$

From this expression we calculate the electric field at $r=a^+$, i.e., just outside the sphere, using continuity conditions (note that the right-hand side is taken at $r=a^-$, not $r=a^+$)

$$\begin{aligned}&\mathbf{E}(r=a^+,\theta)\\ &\quad= -\sum_{l,m=0}\frac{s}{s-s_l}\langle\psi_{lm}|\psi_0\rangle\left(\frac{\epsilon_1}{\epsilon_2}\frac{\partial\psi_{lm}}{\partial r}\hat{\mathbf{r}}+\frac{1}{r}\frac{\partial\psi_{lm}}{\partial\theta}\hat{\boldsymbol{\theta}}\right)_{r=a^-}.\end{aligned}\tag{3.2}$$

We measure the field at the sphere surface and require that the magnitude of a given field component will be of the same order of magnitude as this field component in near-field imaging so that it can be detected. In near-field imaging the field of an object placed in a uniform medium is measured approximately at the object location. We therefore require that an l component measured at the sphere surface and an l component of $\mathbf{E}_0=-\nabla\psi_0$ measured at the point charge location (each field component is finite) will be approximately equal in magnitude. For a point charge in the presence of a sphere we define $\mathbf{r}_0=z_0\hat{\mathbf{z}}$ as the point charge location and $\mathbf{r}=a^+\hat{\mathbf{z}}$ as the measurement point. For near-field imaging we define the point charge location as $\mathbf{r}_{0\,\text{near field}}=a^+\hat{\mathbf{z}}$ and the measurement point also at $\mathbf{r}=a^+\hat{\mathbf{z}}$ and write

$$\begin{aligned}&\frac{E_{r,l,\,\text{sphere setup}}(\mathbf{r}=a^+\hat{\mathbf{z}},\mathbf{r}_0=z_0\hat{\mathbf{z}})}{E_{r,l,\,\text{uniform medium}}(\mathbf{r}=a^+\hat{\mathbf{z}},\mathbf{r}_{0\,\text{near field}}=a^+\hat{\mathbf{z}})}\\ &\quad=\frac{\frac{\epsilon_2}{\epsilon_1}\frac{ss_l}{s-s_l}\psi_{lm}(\mathbf{r}_0=z_0\hat{\mathbf{z}})\frac{\partial\psi_{lm}}{\partial r}\Big|_{\mathbf{r}=a^-\hat{\mathbf{z}}}}{s_l\psi_{lm}(\mathbf{r}=a^+\hat{\mathbf{z}})\frac{\partial\psi_{lm}}{\partial r}\Big|_{\mathbf{r}=a^-\hat{\mathbf{z}}}}\\ &\quad=\frac{\epsilon_2}{\epsilon_1}\frac{s}{s-s_l}(a/z_0)^{l+1}\simeq 1,\end{aligned}\tag{3.3}$$

where we have used $E_{r,l}(\mathbf{r}=a^-\hat{\mathbf{z}})=E_{r,l}(\mathbf{r}=a^+\hat{\mathbf{z}})$ for a point charge in a uniform medium. Assuming $s\simeq 1/2$ and $s_l-s\simeq 0.0025$ we obtain

$$(a/z_0)^{l+1}\simeq 2(s_l-s)\simeq 0.005,$$

and for $l=10$ we get

$$z_0/a\simeq 1.62.$$

This means that if we assume $\epsilon_1\simeq-\epsilon_2$, $s-s_l\simeq(\epsilon_1-\epsilon_{1l})/4\epsilon_2$ and for $\epsilon_2=1.5$, $\epsilon_1-\epsilon_{1l}\simeq 0.015$, and $z_0/a\lesssim 1.62$, the $l=10$ mode magnitude is equal to or higher than its magnitude when measuring $\mathbf{E}_0$ at the point charge location. The angular half-width of this mode near $\theta=\pi$ calculated using the $l=10$ Legendre polynomial is 0.14 rad, which translates to 4 nm for a sphere with a radius of 30 nm.

We now calculate the point charge location using the spectral content of the electric field on the sphere surface. Our motivation for calculating the source location without knowing its magnitude q is, for example, fluorescence in which the emission strength of the source can be unknown. The electric field at the sphere surface is composed of modes with magnitudes that depend on the point charge location. Thus, the spectral information of the electric field is affected by the point charge location. If $s\approxeq s_l$, the electric field is dominated by this l mode. Alternatively, if the radial component of the electric field on the sphere surface can be measured then by using a spherical harmonics transform defined by

$$F(l,m)=\int E_r Y^*_{lm}d\Omega,\tag{3.4}$$

we can obtain the spectral content of an l,m mode in the expansion of the physical electric field. Note that this transform gives the spectral content since $\int Y_{l'm'}Y^*_{lm}d\Omega=\delta_{ll'}\delta_{mm'}$ and $E_{r,lm}$ has a $Y_{l,m}$ associated with it. To perform the transform we need to choose the coordinate system so that $\theta=0$ points to the point charge location. Since the maximal intensity is always at $\theta=0,\pi$ we must choose between them to define $\theta=0$ according to the s value (see discussion above) or by knowing in which half space the point charge is located. The ratio between the magnitudes of the l_1 and l_2 components of the electric field of a point charge located at $\mathbf{r}_0=z_0\hat{\mathbf{z}}$ is

$$\frac{F(l_1,m=0)}{F(l_2,m=0)}=\frac{l_1+1}{l_2+1}\frac{l_2}{l_1}\frac{s_{l_1}}{s_{l_2}}\frac{s-s_{l_2}}{s-s_{l_1}}a^{l_1-l_2}z_0^{l_2-l_1}.\tag{3.5}$$

Thus, from this ratio we can calculate the point charge location z_0 without knowing its magnitude. Now using z_0, it is straightforward to calculate q from any $F(l,m)$ component. In order for the l mode fields of two point charges q_1 and q_2 located at $z_{01}\hat{\mathbf{z}}$ and $z_{02}\hat{\mathbf{z}}$, respectively, to be comparable in magnitude we can require $0.1\lesssim(q_1/q_2)(z_{02}/z_{01})^{l+1}\lesssim 10$. For example, for the $l=10$ mode assuming $q_1=q_2$ we obtain that for comparable field intensities we must have $0.9\lesssim z_{01}/z_{02}\lesssim 1.11$. Thus, objects in a range of 3 nm along r for a sphere with a radius of 30 nm produce comparable field intensities at the sphere surface.

It should be noted that measuring the electric field on the whole sphere is possible only if the detector has a negligible effect on the incoming field at all the measurement points. When the detector is situated on the half sphere that is closer to the source it will be on the path of the incoming field and may interfere with the field. When $s\approx(s_l+s_{l+1})/2$ the field will peak at $\theta=\pi$ and the object location can be approximated using the field magnitude at the half sphere that is further away from the source. Also, measuring the field on the sphere surface necessitates 3D sampling (scanning the field with a detector in three axes), which is more challenging. This concept of transforming a field on a surface to the spectral plane may be adjusted to setups in which the required measurements are more suited for current experimental techniques. For example, in a setup of a flat slab and a source in a host medium [14,17], measuring the electric field at the slab surface that is further away from the source is both two dimensional and has a negligible effect on the measured field. In such a setup the

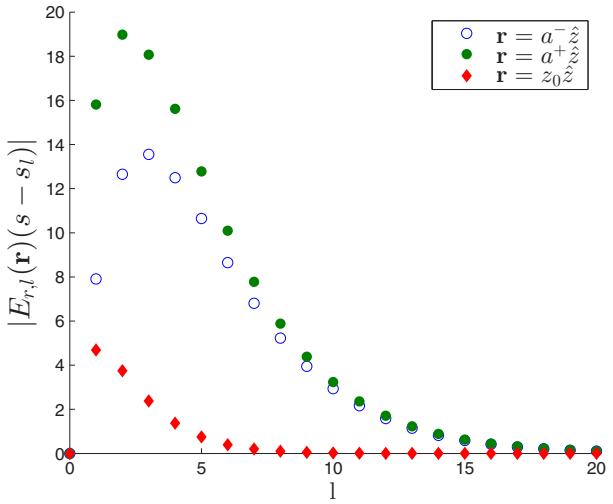

FIG. 1. Plot of $|E_{r,l}(\mathbf{r})(s - s_l)|$ at $\mathbf{r} = a^-\hat{\mathbf{z}}$ and $\mathbf{r} = a^+\hat{\mathbf{z}}$, i.e., just inside and just outside the sphere, and at $\mathbf{r} = z_0\hat{\mathbf{z}}$ as a function of l for $\epsilon_2 = 1$, $z_0 = 1.5a$, and $a = 30$ nm.

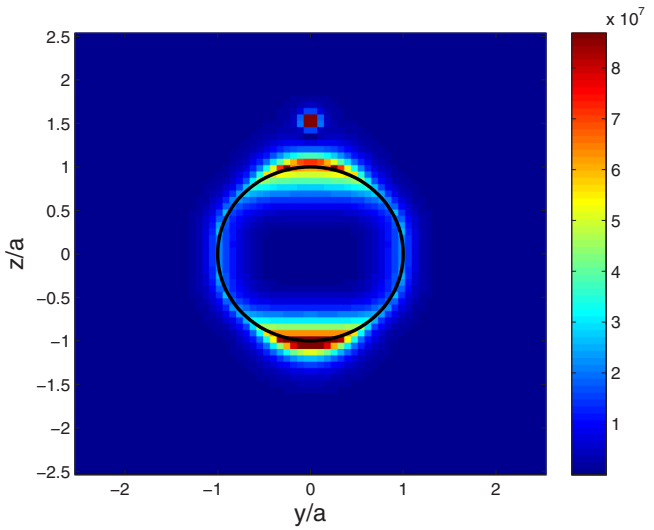

FIG. 2. Plot of $|\mathbf{E}|^2$ for a point charge at $z_0 = 1.5a$, $a = 30$ nm, $s = 0.43$, $\epsilon_2 = 1$, and $\epsilon_1 = -1.3256$.

perpendicular field component at the surface may be Hankel transformed [20] in order to retrieve the source location.

IV. RESULTS

We first considered $\epsilon_2 = 1$ and a point charge located at $z_0 = 1.5a$, where $a = 30$ nm. In order to exclude the effect of the choice of physical s on the results we decomposed each term in the sum in Eq. (2.14) into $(-4\pi q/\epsilon_2)s_l^2\psi^*_{lm}(\mathbf{r}_0)\nabla\psi_{lm}(\mathbf{r})$, which does not depend on the choice of s, and $1/(s - s_l)$. The size of the last factor is determined by the difference between the physical s and the eigenvalue s_l. We calculated

$$|E_{r,l}(\mathbf{r})(s - s_l)| = \left|\frac{4\pi q}{\epsilon_2}s_l^2\psi^*_{l,m=0}(\mathbf{r}_0)\frac{\partial\psi_{l,m=0}(\mathbf{r})}{\partial r}\right| \quad (4.1)$$

at $\mathbf{r} = a^-\hat{\mathbf{z}}$, i.e., just inside the sphere, up to $l = 20$. Note that the spectral components of $\mathbf{E}_0 = -\nabla\psi_0$ can be included in the calculation of $E_{r,l}(\mathbf{r})$ both inside the sphere and at the sphere surface. We found that the $l = 3$ mode with $s_l = 0.4286$ and $\epsilon_{1,l=3} = -4/3$ is the most dominant one. In Fig. 1 we present the results as a function of l.

We then chose $\epsilon_1 = -1.3256$ and $s = 0.43$, which are close to the $l = 3$ mode resonance. We calculated the electric field for these s and ϵ_1 values. The calculation of the electric field was performed analytically using Eq. (2.15). In Fig. 2 we present the intensity of the electric field.

It can be seen that the electric field is significantly enhanced with maximal intensity at the interface between the sphere and the host medium at $\theta = 0,\pi$.

We also calculated $|E_{r,l}(\mathbf{r})(s - s_l)|$ at $\mathbf{r} = a^+\hat{\mathbf{z}}$, i.e., just outside the sphere, and at the point charge location $\mathbf{r} = 1.5a\hat{\mathbf{z}}$ (see Fig. 1). The field intensity at the point charge location is relevant for phenomena such as enhancement of spontaneous emission of a molecule by an antenna and Raman spectroscopy, which become more dominant as the intensity at the molecule increases. The most dominant modes at $\mathbf{r} = a^+\hat{\mathbf{z}}$ and at the point charge location $\mathbf{r} = 1.5a\hat{\mathbf{z}}$ are $l = 2$ and $l = 1$, respectively. The contributions to the electric field inside and outside the sphere do not need to have the same l dependence since continuity of D_r for each mode is satisfied for the eigenvalue ϵ_{1l} but not for ϵ_1.

We then calculated $|E_{r,l}(\mathbf{r})(s - s_l)|$ for $z_0 = 2a$. The most dominant modes of the electric field at $\mathbf{r} = a^-\hat{\mathbf{z}}$ and $\mathbf{r} = a^+\hat{\mathbf{z}}$ and at the point charge location $\mathbf{r} = 2a\hat{\mathbf{z}}$ were found to be $l = 2$, 1, and 1, respectively.

Then, for a point charge located at $\mathbf{r}_0 = 1.15a\hat{\mathbf{z}}$ we calculated $|E_{r,l}(\mathbf{r})(s - s_l)|$ at both $\mathbf{r} = a^-\hat{\mathbf{z}}$ and $\mathbf{r} = a^+\hat{\mathbf{z}}$ and at the point charge location $\mathbf{r} = 1.15a\hat{\mathbf{z}}$, and the most dominant modes were found to be $l = 8$, 7, and 3, respectively (see Fig. 3). Thus, as the point charge approaches the sphere interface the most dominant modes are of higher order, including for a measurement at the point charge location. These calculations necessitated 50 modes in the expansion. Here we were interested to excite high-order modes and compromise on intensity, which is high anyway. We therefore chose $s = 0.487$,

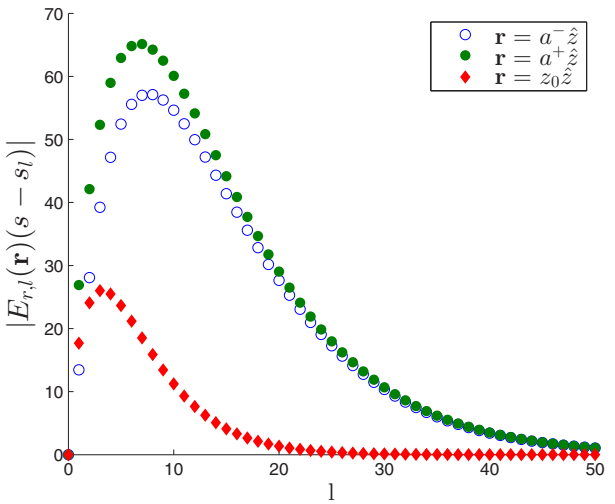

FIG. 3. Plot of $|E_{r,l}(\mathbf{r})(s - s_l)|$ at $\mathbf{r} = a\hat{\mathbf{z}}$ inside and outside the sphere and at $\mathbf{r} = z_0\hat{\mathbf{z}}$ as a function of l for $\epsilon_2 = 1$, a point charge located at $z_0 = 1.15a$, and $a = 30$ nm.

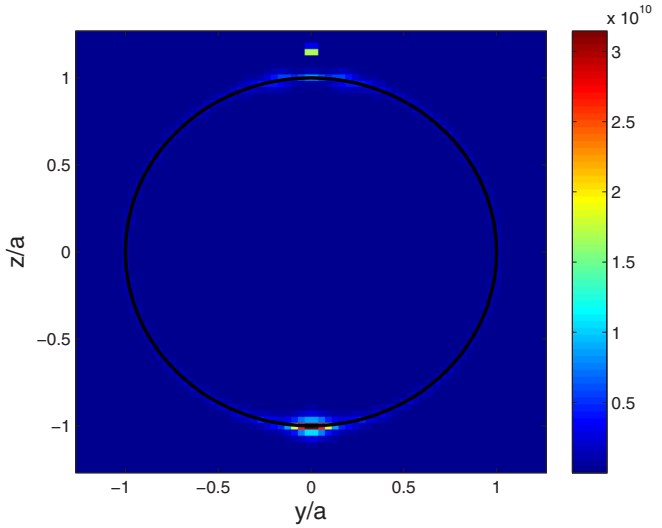

FIG. 4. Plot of $|\mathbf{E}|^2$ for a point charge at $z_0 = 1.15a$, $a = 30$ nm, $s = 0.487$, $\epsilon_2 = 1$, and $\epsilon_1 = -1.0534$.

which corresponds to $\epsilon_1 = -1.0534$ and is in between the $s_{l=19} = 0.4872$ and $s_{l=18} = 0.4865$ resonances. In Fig. 4 we present the electric-field intensity. It can be seen that the field intensity is greatly enhanced. In addition, the field is highly localized at $\theta = \pi$ with $\exp(-1/2)$ of the maximal intensity at $\simeq$2 nm from the maximum.

We were then interested in considering a system that is close the $l = 1$ resonance. The electric field of the $l = 1$ mode extends far from the interface and does not vanish at the origin. A resonance of this mode occurs when the material parameters satisfy $\epsilon_2 \approx -\epsilon_1/2$ and with small and positive $\mathrm{Im}(\epsilon_1)$ and $\mathrm{Im}(\epsilon_2)$ we can approach this resonance. Note that a resonance occurs when $s = s_l$ and the effect of approaching the resonance can be computed by calculating $s_l^2/(s - s_l)$ (see the discussion in Sec. II). We chose $\epsilon_1 = -3.38 + 0.192i$ (silver at 380 nm) and $\epsilon_2 = 1.69 + 0.08i$ and placed a point charge at $\mathbf{r}_0 = 2a\hat{\mathbf{z}}$. In Fig. 5 we present $|\mathbf{E}|^2$ in space. It can be seen that

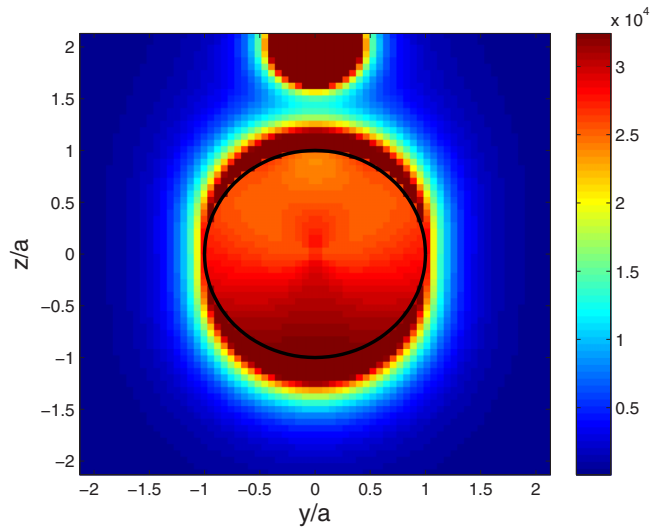

FIG. 5. Plot of $|\mathbf{E}|^2$ for a point charge at $z_0 = 2a$, $a = 30$ nm, $s = 1/3$, $\epsilon_2 = 1.69 + 0.08i$, and $\epsilon_1 = -3.38 + 0.192i$.

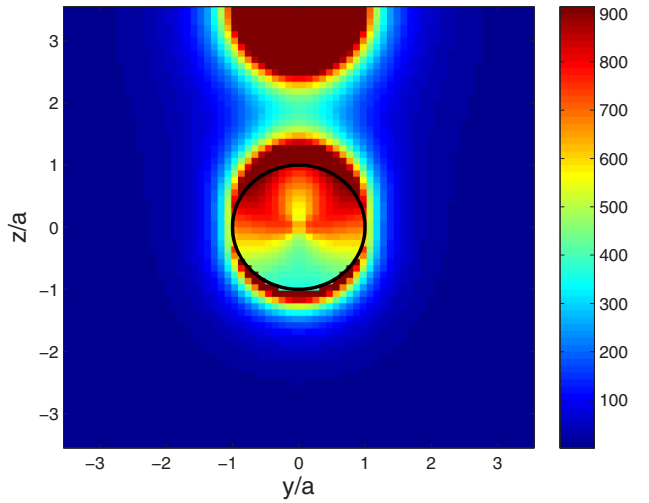

FIG. 6. Plot of $|\mathbf{E}|^2$ for a point charge at $z_0 = 3.5a$, $a = 30$ nm, $s = 0.3$, $\epsilon_2 = 1$, and $\epsilon_1 = -2.33$.

there is a strong electric field inside the sphere even though it is a conductor. Interestingly, water permittivity at 380 nm is $\epsilon_2 = 1.797 + 8.5 \times 10^{-9}$ and a strong electric field inside and outside the sphere is expected for a silver nanosphere immersed in water.

Finally, we calculated $|\mathbf{E}|^2$ for setups in which s is smaller or larger than s_l of all the dominant modes. In these setups the low- and high-order modes interfere constructively at $\theta = 0$. In Fig. 6 we present $|\mathbf{E}|^2$ for $z_0 = 3.5a$ and $s = 0.3$ ($\epsilon_2 = 1$ and $\epsilon_1 = -2.33$), which is smaller than all the eigenvalues s_l. It can be seen that the intensity is strong at $\theta = 0$ and that the electric field extends far from the sphere surface since s is closer to s_l of the low-order modes. In Fig. 7 we present $|\mathbf{E}|^2$ for $z_0 = 1.5a$ and $s = 0.492$ ($\epsilon_2 = 1$ and $\epsilon_1 = -1.0325$), which is larger than the eigenvalues s_l of the dominant modes. The intensity is again strong at $\theta = 0$ and is spatially concentrated since s is closer to s_l of the high-order modes that are associated with high spatial frequencies.

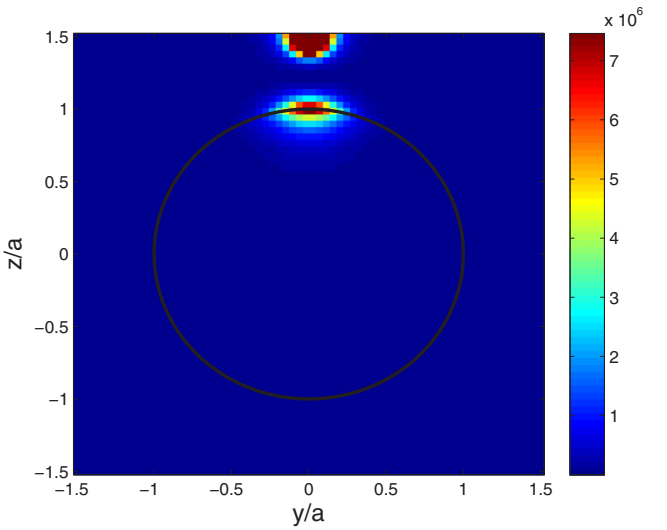

FIG. 7. Plot of $|\mathbf{E}|^2$ for a point charge at $z_0 = 1.5a$, $a = 30$ nm, $s = 0.492$, $\epsilon_2 = 1$, and $\epsilon_1 = -1.0325$.

To verify our results we checked the continuity of the physical D_r at the interface. In the electric-field expansions $\mathbf{E}_0$ is continuous and all the eigenstates satisfy continuity of D_r with their ϵ_{1l} eigenvalue. Thus, none of the terms in the expansion is expected to satisfy continuity of physical D_r at the interface. Our calculations showed that the physical D_r is continuous at the interface for various s values to a high accuracy.

The calculations were performed using a grid of 70×70 on the y and z axes. In our calculations of the potential and the electric field in all space, the running times on a single core were ~2, 3, and 8 s for $z_0 = 2a$, $1.5a$, and $1.15a$, respectively, which can be reduced by an order of magnitude with code optimization in MATLAB.

V. DISCUSSION

We presented an analytic expansion of the potential and the electric field for a setup of an ϵ_1 sphere embedded in an ϵ_2 host medium, where the permittivity values of the sphere and the host medium can take any value. For a point charge on the z axis at z_0 the expansion only includes the $m = 0$ terms and involves up to 20 terms when $z_0 \gtrsim 1.5a$. For a given charge location and measurement point a dominant mode can be readily identified and one can select a sphere permittivity value that is close to the mode resonance in order to obtain a significant enhancement of the electric field.

We placed a point charge at $z_0 = 1.5a$, $1.15a$, $2a$, and $3.5a$ and chose permittivity values that are close to a resonance. We observed very high enhancement of the electric field. Interestingly, a significant electric field can exist inside the sphere even if it is a conductor, when ϵ_1/ϵ_2 is close to $(\epsilon_1/\epsilon_2)_l$ of a dominant mode. The contribution of the high-order modes becomes non-negligible as the point charge approaches the sphere surface. The low-order modes decay more slowly and generate an electric field away from the surface. Very high resolution is obtained when a high-order mode is excited since high-order modes are associated with high spatial frequencies. When $s \approx (s_l + s_{l+1})/2$ the dominant l and $l+1$ modes interfere constructively at $\theta = \pi$. When $\epsilon_1 \gtrsim -2\epsilon_2$, the radial field component of all the modes at $\theta = 0$ interfere constructively and generate a strong signal dominated by the low-order modes that extend far from the sphere surface. Similarly, when $\epsilon_1 \lesssim -\epsilon_2$ the radial field component of all the modes at $\theta = 0$ interfere constructively and a strong signal dominated by the high-order modes that are associated with high spatial frequencies is generated.

We showed that the spectral information at the sphere surface can be utilized to calculate the point charge location without knowing its magnitude. In addition, when the system is close to a resonance the high-order modes of the electric field can be retrieved. These may have relevance for near-field imaging of objects that are not at the surface. To assist in balancing the smaller magnitudes of evanescent waves from distant sources, the magnitude of the light sources can be larger for larger r, which can be achieved by back illumination. Gain can both enhance the incoming field and enable s that is closer to the s_l resonances that are real. Another possible mechanism to enable detection of high-order modes in the expansion of the electric field of a point charge that is not very close to the surface is to mediate them through resonant particles inside the medium that enhance them, similarly to the isolated sphere. Since we can calculate the point charge location for a single point charge, selectively exciting local points that radiate at different times may enable one to retrieve their locations too [21,22]. A similar analysis can be formulated for a setup of a flat slab in a host medium [14] where the spectrum of the eigenvalues is continuous.

Potential applications are enhancement of spontaneous emission of a molecule by an antenna [18], where the point charge and the sphere can model the molecule and the antenna, respectively, sensing, modeling a tip in proximity to a metallic nanosphere, near-field imaging, and Raman spectroscopy. Finally, since the expansion employs a small number of terms for a single point charge source, calculating the potential and the electric field in all space is very fast.

[1] J. D. Jackson, *Electrodynamics* (Wiley, New York, 1975).
[2] J. A. Stratton, *Electromagnetic Theory* (McGraw-Hill, New York, 1941).
[3] F. García-Moliner and F. Flores, *Introduction to the Theory of Solid Surfaces* (Cambridge University Press, Cambridge, 2009).
[4] B. van der Pol and H. Bremmer, Philos. Mag. **24**, 141 (1937).
[5] H. Chew, P. McNulty, and M. Kerker, Phys. Rev. A **13**, 396 (1976).
[6] J. Gersten and A. Nitzan, J. Chem. Phys. **95**, 686 (1991).
[7] N. A. Nicorovici, R. C. McPhedran, and G. W. Milton, Phys. Rev. B **49**, 8479 (1994).
[8] G. W. Milton, N.-A. P. Nicorovici, R. C. McPhedran, and V. A. Podolskiy, Proc. R. Soc. A **461**, 3999 (2005).
[9] G. W. Milton and N.-A. P. Nicorovici, Proc. R. Soc. A **462**, 3027 (2006).
[10] H. Kettunen, M. Lassas, and P. Ola, arXiv:1406.6224.
[11] D. J. Bergman, J. Phys. C **12**, 4947 (1979).
[12] D. J. Bergman, Phys. Rev. B **19**, 2359 (1979).
[13] D. J. Bergman, Phys. Rev. A **89**, 015801 (2014).
[14] A. Farhi and D. J. Bergman, Phys. Rev. A **90**, 013806 (2014).
[15] D. J. Bergman, in *Les Méthodes de l'Homogénéisation: Théorie et Applications en Physiques*, edited by R. Dautray (Editions Eyrolles, Paris, 1985), pp. 1–128.
[16] D. J. Bergman and D. Stroud, Phys. Rev. B **22**, 3527 (1980).
[17] A. Farhi and D. J. Bergman, Phys. Rev. A **93**, 063844 (2016).
[18] M. S. Eggleston, K. Messer, L. Zhang, E. Yablonovitch, and M. C. Wu, Proc. Natl. Acad. Sci. USA **112**, 1704 (2015).
[19] A. R. Edmonds, *Angular Momentum in Quantum Mechanics* (Princeton University Press, Princeton, 1957).
[20] R. N. Bracewell and R. N. Bracewell, *The Fourier Transform and its Applications* (McGraw-Hill, New York, 1986), Vol. 31999.
[21] J. Hanne, H. J. Falk, F. Görlitz, P. Hoyer, J. Engelhardt, S. J. Sahl, and S. W. Hell, Nat. Commun. **6**, 7127 (2015).
[22] M. Fernández-Suárez and A. Y. Ting, Nat. Rev. Mol. Cell Biol. **9**, 929 (2008).